1

Intracellular BH3 profiling reveals shifts in anti-apoptotic dependency in B-cell maturation and activation

Joanne Dai[1] and Micah A. Luftig[1,*]

[1] Department of Molecular Genetics and Microbiology, Center for Virology, Duke University School of Medicine, Durham, NC, 27710, USA

*Corresponding author: Micah A. Luftig, Department of Molecular Genetics and Microbiology, Center for Virology, Duke University School of Medicine, Durham, NC, 27710, USA; 919-668-3091; email: micah.luftig@duke.edu

Keywords: B cell, Apoptosis, iBH3 Profiling, BH3 Mimetics

Short Title: iBH3 profiling of normal and activated B-cell subsets

15 **Abstract**

16   Apoptosis is critical to B-cell maturation, but studies of apoptotic regulation in primary

17   human B cells is lacking. Previously, we found that infecting human B cells with Epstein-Barr

18   virus induces two different survival strategies (Price *et al.*, 2017). Here, we sought to better

19   understand the mechanisms of apoptotic regulation in normal and activated B cells. Using

20   intracellular BH3 profiling (iBH3), we defined the Bcl2-dependency of B-cell subsets from human

21   peripheral blood and tonsillar lymphoid tissue as well as mitogen-activated B cells. We found

22   that naïve and memory B cells were BCL-2 dependent, while germinal center B cells were MCL-

23   1 dependent and plasma cells were BCL-XL dependent. Proliferating B cells activated by CpG

24   or CD40L/IL-4 became more dependent upon MCL-1 and BCL-XL. As B-cell lymphomas often

25   rely on survival mechanisms derived from normal and activated B cells, these findings offer new

26   insight into potential therapeutic strategies for lymphomas.

27

Introduction

The maturation of B cells into antibody-secreting cells is critical to immunity and is accomplished through either T-independent or T-dependent B-cell maturation. In T-independent B-cell maturation, antigen binding to the B-cell receptor (BCR) stimulates extra-follicular naïve and memory B cells to proliferate (Bortnick and Allman, 2013). B cells can also be activated via pathogen-associated molecular patterns (PAMPs), like CpG DNA, binding to Toll-like receptors (TLR) (Bernasconi et al., 2002; Krieg et al., 1995). Activated B cells can differentiate into short-lived plasmablasts or migrate into secondary lymphoid tissue to undergo T-dependent maturation. In the germinal center (GC) reaction, the affinity for antigen is further refined through somatic hypermutation and selection by apoptosis (Victora and Nussenzweig, 2012). B cells also compete for survival signals in the form of antigen binding to the BCR and CD40 receptor binding by to cognate T follicular helper cells. Outcompeted B cells are eliminated by apoptosis and surviving B cells exit the GC as long-lived memory B cells or plasma cells.

Ultimately, the humoral repertoire is shaped by apoptosis dependent on the multi-domain Bcl-2 family proteins that select which B cells die and which continue to propagate (Peperzak et al., 2012). Apoptosis is initiated when BAX and BAK dimerize and permeabilize the mitochondrial outer membrane to release cytochrome C into the cytosol, which activates a cascade of caspases that mediate DNA fragmentation, protein degradation, and cellular blebbing (Fischer et al., 2003). To prevent aberrant activation, anti-apoptotic proteins bind and sequester BAX and BAK as well as the pro-apoptotic BH3-only proteins (named as such because they share homology in their BH3 domain). Dysregulation of apoptosis typically accompanies the development of lymphomas or autoimmunity, and understanding the mechanisms of apoptosis regulation is key to provide insight and develop new therapeutic strategies for these diseases (Vo et al., 2012).

3

52   New breakthroughs in studying apoptosis regulation during B-cell maturation have been

53   made possible by the development of BH3 mimetics, a class of small molecular inhibitors that

54   mimic pro-apoptotic proteins and have shown great promise as cancer therapeutics (Oltersdorf

55   et al., 2005). In mice, naïve and memory B cells are sensitive to the BH3 mimetic ABT-737,

56   which inhibits BCL-2, BCL-XL, and BCL-W, but pre-existing GC and plasma cells are resistant

57   (Carrington et al., 2010), suggesting that apoptosis is regulated differently at various stages of

58   B-cell maturation. Recently, human tonsillar GC B cells were found to be sensitive to MCL-1

59   inhibition, which supports previous findings that MCL-1 is essential for GC formation in mice

60   (Peperzak et al., 2017; Vikstrom et al., 2010). Nonetheless, there remain challenges associated

61   with studying apoptosis in primary human B cells, which have short life-spans in culture,

62   spontaneously undergo apoptosis, and are difficult to transfect. In addition, how apoptotic

63   regulation changes specifically during B-cell activation poorly understood. As a result, we

64   utilized intracellular BH3 (iBH3) profiling to uncover the dominant anti-apoptotic mechanism at

65   the mitochondria of resting and activated primary human B cells. The principles behind iBH3

66   profiling are based upon the selective interactions between the pro- and anti-apoptotic proteins

67   of the Bcl2-family (Deng et al., 2007; Youle and Strasser, 2008). In short, the anti-apoptotic

68   proteins that are present at the mitochondria dictate which pro-apoptotic BH3-only peptides can

69   induce mitochondrial depolarization and cytochrome C release. In this way, we can identify the

70   anti-apoptotic dependency, or Bcl2-depedency, of the sample. iBH3 profiling can also assay the

71   Bcl2-dependency of multiple populations in heterogeneous samples, thereby eliminating the

72   need for time-consuming and expensive sorting experiments to study rare populations (Ryan et

73   al., 2016).

74   With the advent of iBH3 profiling and BH3 mimetics, we are equipped with tools that

75   allow us to study how apoptosis is regulated in human B-cell subsets and activated B

76   cells. Therefore, we have used iBH3 profiling to determine the BH3 profiles of normal, resting,

77 and activated B cells, and validated the hypotheses generated by these profiles by treating

78 normal and activated human B-cell subsets with BH3 mimetics.

79

80 **Results**

81 **Naïve and memory B cells circulating in the periphery depend upon BCL-2 for survival**

82 To ensure the reliability of iBH3 profiling, we sought to determine the mechanism of

83 apoptosis regulation in peripheral blood B cells from within the bulk PBMC population

84 (Carrington et al., 2010). After staining for cell-specific surface markers, cells were incubated

85 with recombinant BH3-only peptides and digitonin, which selectively permeabilizes the outer

86 cellular membrane and exposes intact mitochondria to the peptide treatment (**Figure 1A**).

87 Following peptide treatment, the cells were fixed, incubated with saponin to permeabilize

88 mitochondria, and stained with a fluorescently-labeled antibody to quantify the remaining levels

89 of intracellular cytochrome C. The extent of cytochrome C release was measured as the

90 dynamic range between total levels of cytochrome C, determined by treating with an inert

91 recombinant PUMA BH3-only peptide (PUMA2A) and alamethicin (Alm), which can induce

92 100% cytochrome C release.

93 Naïve (CD19$^+$ IgD$^+$) and memory (CD19$^+$ IgD$^-$) B cells were distinguished by IgD

94 expression (**Figure 1B**). iBH3 profiling revealed that the mitochondria in naïve and memory B

95 cells in the peripheral blood were highly sensitive to BIM, BAD, PUMA, and BMF, and relatively

96 resistant to NOXA and HRK (**Figure 1C**). This pattern of sensitivity suggested that naïve and

97 memory B cells were dependent upon BCL-2 for survival (**Figure 1D**).

98 To validate this hypothesis, we treated PBMCs with the following BH3 mimetics: ABT-

99 737 (BCL-2, BCL-XL, BCL-W inhibitor), ABT-199 (BCL-2 inhibitor), or WEHI-539 (BCL-XL

100 inhibitor) (**Figure 1E**). Naïve and memory B cells were resistant to WEHI-539 (IC$_{50}$ >1 μM) and

101   were sensitive to ABT-737 and ABT-199 (IC_{50} <1 μM), thereby confirming our iBH3 profiling

102   hypotheses and previously published results of BCL-2 dependency (**Figure 1F**). ABT-199 was

103   used to distinguish between BCL-2 and BCL-W, which have identical binding partners (**Figure**

104   **1D**). Staurosporine (STS) is not a BH3 mimetic, but rather it is a pan-kinase inhibitor that

105   induces apoptosis and was used here to distinguish cells that can undergo apoptosis from those

106   that can't, such as cells that lack the effector molecules BAX and BAK (Wei et al., 2001).

B-cell maturation is associated with changes in Bcl-2 family dependency

108   To determine the changes in apoptotic regulation that take place during human B-cell

109   maturation, we queried the apoptotic regulation of $CD19^+$ naïve (IgD^+ $CD38^-$), memory (IgD^-

110     $CD38^-$), germinal center (GC; IgD^- $CD38^{mid}$) B cells, and plasma cells (IgD^- $CD38^{hi}$) from tonsillar

111   tissue (**Figure 2A**). Like naïve and memory B cells in peripheral blood, tonsillar naïve and

112   memory B cells were highly sensitive to BIM, BAD, PUMA, and BMF and were predicted to be

113   BCL-2 dependent (**Figure 2B-C**). GC B cells, however, had a modestly lower response to BAD

114   and a heightened response to NOXA, suggesting that GC B cells were dependent upon MCL-1

115   for survival. Plasma cells were much less responsive to BH3 peptide treatments compared to

116   the other B-cell subsets. However, we hypothesized that within the reduced dynamic range of

117   plasma cell responses, lower NOXA sensitivity as compared to BAD and HRK suggested

118   dependence on BCL-XL for survival.

119   To validate the hypotheses generated from iBH3 profiling, we treated primary tonsillar B

120   cells with ABT-199, ABT-737, WEHI-539, and STS (**Figure 2D-E**). All cells were sensitive to

121   STS, indicating that all subsets were capable of intrinsic apoptosis. As predicted, naïve and

122   memory B cells were sensitive to BCL-2 inhibition by ABT-199 and ABT-737. Plasma cells were

123   uniquely sensitive to BCL-XL inhibition by WEHI-539, confirming their dependence on BCL-XL.

124   The difference in the sensitivity of plasma cells to ABT-737 and WEHI-539 may be due to a

125   difference in their binding affinities for BCL-XL (ABT-737 IC_{50}=35nM vs WEHI-539 IC_{50}=1.1nM)

126   (Lessene et al., 2013; Oltersdorf et al., 2005). GC B cells were resistant to ABT-737, ABT-199,

127   and WEHI-539 since none of these drugs inhibited MCL-1. However, GC B cells were also

128   resistant to the MCL-1 specific BH3 mimetic, A-1210477 (**Figure 2 Figure Supplement 1**),

129   which is likely due to its weak cellular potency (i.e. sensitivity in the micromolar range) and

130   nonspecific toxicity (Kotschy et al., 2016; Leverson et al., 2015). In sum, these findings support

131   an existing model that B cells adjust their Bcl-2 family dependency throughout T-dependent B

132   cell maturation. Moreover, iBH3 profiling proved to be reliable in querying heterogeneous

133   populations simultaneously.

134   **CD40L/IL-4 stimulated B cells are sensitive to NOXA and HRK peptides, yet remain**

135   **sensitive to BCL-2 inhibition**

136   We next sought to model B-cell maturation with mitogen stimulation of peripheral blood

137   B cells. To track proliferation, PBMCs were stained with CellTrace Violet (CTV), which becomes

138   diluted upon cell division (**Figure 3A**). CTV was retained during permeabilization with digitonin,

139   thereby making it suitable in iBH3 profiling. We induced proliferation in peripheral blood B cells

140   *ex vivo* by treating with CD40L and IL-4 to mimic T-cell derived signals important in B-cell

141   survival in the GC. CD19+ B cells began proliferating 3 days after treatment with CD40L/IL-4, as

142   shown previously (Hawkins et al., 2007; Nikitin et al., 2014).

143   CD40L/IL-4 stimulated B cells were iBH3 profiled six days post-stimulation (**Figure 3B**).

144   Proliferating B cells displayed modestly increased sensitivity to NOXA and HRK peptide

145   treatment relative to nonproliferating B cells, suggesting an increasing dependence on MCL-1

146   and BCL-XL for survival. The robust increase in HRK sensitivity correlated with increased

147   susceptibility of proliferating B cells to the BCL-XL inhibitor, WEHI-539 (**Figure 3C-D**). However,

148   these cells remained sensitive to ABT-199 and ABT-737, suggesting that BCL-2 still plays an

149   important role in CD40L/IL-4 stimulated B-cell survival (**Figure 3C-D**). This also indicates that

150   NOXA sensitivity observed in proliferating B cells did not confer MCL-1 dependence.

7

151 **A CD38^{hi}, plasmablast-like subpopulation in CpG-stimulated B cells becomes sensitive to**

152 **NOXA and HRK in iBH3 profiling and becomes resistant to BCL-2 inhibition**

153   In B cells activated to proliferate *ex vivo* by CpG DNA, a PAMP that stimulates the TLR9

154 pathway, we observed similar changes in apoptotic regulation in proliferating B cells. However,

155 in CpG-stimulated cells, B cells that have undergone the most cellular divisions upregulate high

156 levels of CD38 surface expression, suggesting that they have differentiated into plasmablast-like

157 B cells (CTV^{lo} CD38^{hi}; **Figure 4A**) (Bernasconi et al., 2002; Huggins et al., 2007). This

158 population consisted predominantly of memory B cells and is noticeably absent in CD40L/IL-4

159 stimulated B cells because IL-4 downregulates CD38 expression through serine/threonine

160 kinases (Shubinsky and Schlesinger, 1996). In iBH3 profiling of CpG-stimulated B cells,

161 nonproliferating B cells were predicted to be BCL-2 dependent and as they proliferate they

162 become more responsive to NOXA and HRK peptides with CD38^{hi} B cells as the most

163 responsive to NOXA and HRK (**Figure 4B**).

164   Nonproliferating and CD38^{lo} proliferating B cells were within the same range of

165 sensitivity to ABT-199 and ABT-737 and were refractory to WEHI-539, indicating that as B cells

166 proliferated in response to CpG, BCL-2 remained important in regulating survival (**Figure 4C-D**).

167 CD38^{hi} B cells, in contrast, were less sensitive to ABT-199, ABT-737, and slightly more sensitive

168 to WEHI-539. Interestingly, it appeared that WEHI-539 increased the number of proliferating

169 CD38^{lo} memory B cells (**Figure 4C**), suggesting that in T-independent B-cell maturation, BCL-

170 XL may be involved in the differentiation of plasmablasts derived from memory B cells. This also

171 indicates that the perceived sensitivity of the CD38^{hi} cells to WEHI-539 may not be due to cell

172 death, but rather from a block in differentiation.

173   The overall increase in apoptosis resistance in the CD38^{hi} subset is not because of

174 impaired BAX and BAK activation, since CD38^{hi} cells were sensitive to STS, but rather it may be

175 due to an increasing dependence upon MCL-1 as indicated by increasing sensitivity to NOXA in

8

176   their iBH3 profile. In fact, of the proliferating subsets, only the response of the CD38^{hi} subset to

177   NOXA was significantly different from that of nonproliferating B cells (* p=0.0292). Thus, to

178   inhibit both BCL-XL and MCL-1, we tested the efficacy of combining WEHI-539 with A-1210477

179   in CpG-stimulated PBMCs (Chou, 2010). CpG-stimulated B cells were refractory to high

180   concentrations of A-1210477 (**Figure 4 Figure Supplement 1A-B**). However, a combination of

181   A-1210477 and sub-IC$_{50}$ levels of WEHI-539 resulted in synergism (Combination Index, CI<1) in

182   the CD38^{hi} subpopulation (**Figure 4 Figure Supplement 1C**). This effect was specific to MCL-1

183   as ABT-199 did not synergize with WEHI-539 (CI≈1) (**Figure 4 Figure Supplement 1D**).

184

185   **Discussion**

186   Proper regulation of apoptosis is critical for B-lymphocyte development and maturation.

187   Much of our mechanistic understanding of B-cell apoptosis is derived from murine studies due

188   to technical limitations in studying B-cell subsets in humans (Carrington et al., 2010; Peperzak

189   et al., 2013; Vikstrom et al., 2010). While two recent studies have characterized Bcl-2 family

190   dependency in human primary and secondary lymphoid tissue (Peperzak et al., 2017; Sarosiek

191   et al., 2017), in this study we use the newly developed iBH3 profiling technique to query the

192   mechanisms underlying apoptotic regulation both in heterogeneous lymphoid tissue as well as

193   upon activation of normal B-cell subsets *ex vivo* (Ryan and Letai, 2013; Ryan et al., 2016). Our

194   experimental approach couples proliferation tracking with cell surface markers to measurement

195   of intracellular cytochrome C release in response to BH3 peptides to define Bcl2 family member

196   dependency at the single cell level during B-cell activation. Validation of iBH3 profiling with BH3

197   mimetics defined transitions during B-cell maturation from BCL-2 dependency in naïve and

198   memory B cells, to MCL-1 in GC B cells, and to BCL-XL in plasma cells from secondary

199   lymphoid tissue. Then, upon activation by CpG or CD40L/IL-4, the Bcl2-dependency of

200   proliferating B cells shifts from BCL-2 to a combination of BCL-XL and MCL-1. This shift is

201   apparent by the increased resistance to BCL2-specific BH3 mimetics and is most pronounced in

202   the most differentiated subset of CpG-stimulated B cells.

203   Our findings corroborate several *in vivo* studies in mice that suggest that stage-specific

204   Bcl2-dependency occurs throughout B-cell maturation. Our work indicates that human naïve

205   and memory B cells, like those in mice, are sensitive to BCL-2 inhibition, whereas GC and

206   plasma cells are refractory (Carrington et al., 2010). In mouse GC B cells or those induced to

207   differentiate into plasma cells *ex vivo*, MCL-1 is important in promoting survival (Peperzak et al.,

208   2013; Vikstrom et al., 2010). Furthermore, murine plasma cells depend on BCL-XL protection

209   from apoptosis due to the unfolded protein response (Gaudette et al., 2014). These parallels in

210   mouse studies with our findings in human B cells suggest that intrinsic apoptotic regulation in B-

211   cell maturation is highly conserved and functionally critical to humoral immunity.

212   Proliferating B cells in the GC as well as *ex vivo* mitogen-stimulated B blasts display

213   evidence of oxidative and metabolic stress as well as DNA damage, which if left unresolved can

214   lead to apoptosis (Jellusova et al., 2017; Nikitin et al., 2014; Ranuncolo et al., 2007; Wheeler

215   and Defranco, 2012). Our findings indicate that GC cells display a heightened response to

216   NOXA in iBH3 profiling suggesting an increased dependence on MCL-1. In addition, our lab has

217   found that following EBV infection of primary human B cells, which is characterized by

218   hyperproliferation and activation of the DNA damage response (Nikitin et al., 2010), there is a

219   shift in Bcl2-dependency from BCL-2 to MCL-1 (Price et al., 2017). This suggests that upon

220   proliferation, MCL-1 expression is rapidly induced to respond to apoptosis-inducing intracellular

221   stress resulting from rapid expansion and differentiation.

222   Constitutive activation of gene expression and survival programs found in normal B-cell

223   maturation can promote the development of lymphomas. For example, in follicular lymphoma, a

224   t(14;18) chromosomal translocation induces BCL-2 over-expression in naïve B cells thereby

225   promoting survival in the B-cell follicle of a GC (Kridel et al., 2012; Tsujimoto et al., 1985).

226   Consistent with our findings and that of others linking GC survival to MCL-1 up-regulation

227   (Peperzak et al., 2017; Vikstrom et al., 2010), a subset of DLBCLs that arise from the GC often

228   display MCL-1 copy number gains (Wenzel et al., 2013). Indeed, c-Myc-driven Burkitt's

229   lymphomas are thought to have arisen from GC B cells, express high levels of MCL-1 and are

230   sensitive to MCL-1 inhibition (Dave et al., 2006; Kelly et al., 2014; Klein et al., 1995; Kotschy et

231   al., 2016). MCL-1 is also often over-expressed in plasma-cell derived multiple myelomas,

232   mimicking the requisite up-regulation of MCL-1 induced by stromal interactions in the bone

233   marrow (Gupta et al., 2017; Wuilleme-Toumi et al., 2005). Interestingly, a subset of plasma-cell

234   derived tumors also display co-dependence of MCL-1 and BCL-XL (Morales et al., 2011),

235   similar to our findings in CpG-induced CD38^{hi} plasmablasts. Overall, these data strongly support

236   the importance of defining normal and activated human B-cell survival mechanisms towards

237   understanding the underlying basis of B-lymphoma cell survival.

238

239

11

240 **Materials and Methods**

241 **Cells and mitogens**

242   Peripheral B cells were obtained from normal human donors through the Gulf Coast

243 Regional Blood Center (Houston, TX). Buffy coats were layered over Ficoll Histopaque-1077

244 gradient (Sigma, H8889) and washed three times with FACS buffer (5% FBS in PBS) and

245 cultured in RPMI supplemented with 15% FBS (Corning), 2 mM L-Glutamine, 100 U/ml

246 penicillin, 100 μg/ml streptomycin (Invitrogen), and cyclosporin A. To track proliferation, PBMCs

247 were stained with CellTrace Violet (Invitrogen, C34557) for 20min in PBS at 37°C, washed in

248 FACS buffer, and then cultured with the appropriate mitogens.

249   Tonsillar B cell subsets were obtained from discarded, anonymized tonsillectomies from

250 the Duke Biospecimen Repository and Processing Core (Durham, NC). Tonsillectomies were

251 manually disaggregated, filtered through a cell strainer, and isolated by Ficoll Histopaque-1077

252 (Sigma, H8889). The harvested lymphocyte layer was washed three times with FACS buffer and

253 cultured in RPMI supplemented with 15% FBS (Corning), 2 mM L-Glutamine, 100 U/ml

254 penicillin, 100 μg/ml streptomycin (Invitrogen), and cyclosporin A.

255   TLR9 ligand CpG oligonucleotide (ODN 2006) was purchased from IDT and used at 2.5

256 μg/mL (Krieg et al., 1995). Human recombinant interleukin-4 (IL-4; Peprotech, AF200-04) was

257 used at 20ng/mL. HA-tagged CD40 ligand (R&D Systems, 6420-CL) was used at 5ng/mL with

258 an anti-HA cross-linking peptide (R&D Systems, MAB060; RRID:AB_10719128) at a

259 concentration of 0.2 μg/μL.

260 **Intracellular BH3 profiling and validation**

261   Intracellular BH3 (iBH3) profiling was performed with recombinant peptides synthesized

262 by New England Peptides (sequences listed in table). Stock peptides were resuspended at

263 10mM in DMSO and aliquoted and stored at -80°C. To prepare peptides for iBH3 profiling,

264   peptides were diluted to 200µM in 0.004% digitonin in DTEB buffer (135mM trehalose (Sigma,

265   T9449), 20µM EDTA (Sigma, E6758), 20µM EGTA (Sigma, E3889), 5mM succinic acid (Sigma,

266   S3674), 0.1% IgG-free BSA (VWR, 100182-742), 10mM HEPES (Sigma H4034), 50mM

267   potassium chloride (Sigma, P9541), adjusted to pH 7.5 with potassium hydroxide). Bim peptides

268   were used at 10µM, 1µM, and 0.1µM Alamethicin (Enzo, BML-A150-0005) was used at 25µM.

269   PBMCs and tonsillar cells were iBH3 profiled immediately after processing, while

270   mitogen-stimulated cells were profiled on day 6 post-stimulation. To prepare samples for iBH3

271   profiling, cells were stained with the Zombie Aqua viability dye (Biolegend, 423101) in serum-

272   free PBS for 15min at room temperature and then stained with FACS antibodies for surface

273   markers for 30min at 4°C. Because Zombie Aqua and CellTrace Violet fluoresce in the same

274   channel, mitogen-stimulated cells were centrifuged at low speed and washed to remove dead

275   cells (ie Trypan positive) before staining. After staining, cells were pelleted and resuspended at

276   4×10^6 cells/mL in DTEB buffer. Equal volumes (50µL) of cells and peptides were incubated in

277   polypropylene tubes for 1hr at room temperature in the dark. To stop the reaction, 30µL of 4%

278   PFA in PBS was added and incubated at room temperature for 10min. To neutralize the fixation,

279   30µL of neutralization buffer (1.7M TRIS base, 1.25M glycine, pH 9.1) was added for 5min.

280   Intracellular levels of cytochrome C were probed by adding 20µL of staining buffer (1% saponin,

281   10% BSA, 20% FBS, 0.02% sodium azide in PBS) with 1µL antibody for human cytochrome C.

282   Samples were stained overnight and then transferred into polystyrene tubes for analysis the

283   next day.

Peptide	Amino acid sequence
Bad	Ac-LWAAQRYGRELRRMSDEFEGSFKGL-NH2
Bim	Ac-MRPEIWIAQELRRIGDEFNA-NH2
Bmf	Ac-HQAEVQIARKLQLIADQFHRY-NH2

13

Hrk	Ac-WSSAAQLTAARLKALGDELHQ-NH2
Noxa	Ac-AELPPEFAAQLRKIGDKVYC-NH2
Puma	Ac-EQWAREIGAQLRRMADDLNA-NH2
Puma2A	Ac-EQWAREIGAQARRMAADLNA-NH2

284 Ac – Acetyl, NH2 – Amide.

Flow cytometry

286   To track proliferation, cells were stained with CellTrace Violet (Invitrogen, C34557). Cells

287 were washed in FACS bufer (5% FBS in PBS), stained with fluorescently-conjugated antibodies

288 for 30min-1hr at 4°C in the dark, and then washed again before being analyzed on a BD FACS

289 Canto II. To normalize acquisition, Spherotech Accucount (ACBP-50-10) beads were included in

290 each tube.

Antibodies used for flow-cytometry:		
PE Mouse Anti-Human IgD	BD Pharmingen, 555779	(no RRID)
APC Mouse Anti-Human CD38	Biolegend, 303510	RRID:AB_314362
PECy7 Mouse Anti-Human CD19	eBioscience, 25-0198-42	RRID:AB_10671548
FITC Mouse Anti-Human cytochrome C	Biolegend, 612304	RRID:AB_2090159

291

Dose-response curves and isobolograms

293   Small molecule inhibitors used in this study were ABT-737 (Selleckchem, S1002), ABT-

294 199 (Adooq Biosciences, A12500), WEHI-539 (APExBIO, A3935), A1210477 (Selleckchem,

295 S7790), and staurosporine (Sigma, S5921-0.5MG). Dose-response curves were generated by

296 treating primary cells for 24 hours at 37°C. Mitogen-activated cells were treated on day 3 post-

297 stimulation for 3 days and assayed on day 6. Cell counts were performed by flow cytometry and

14

298 normalized to a DMSO (vehicle only) control. Curves were drawn in GraphPad Prism 7 to

299 calculate IC_{50} values and 95% confidence intervals based on a Hill slope factor of 1.

300 Isobolograms were generated based on dose-response curves with individual drugs

301 (Drug 1, Drug 2) and combinations of drugs (Drug 1 + Drug 2) (Chou, 2010). Individual drug

302 dose-response curves were used to identify drug concentrations at IC_{30}, IC_{50}, and IC_{70}. Similarly,

303 at a constant concentration of Drug 1, the concentrations of Drug 2 were determined at the IC_{30},

304 IC_{50}, and IC_{70} points of the combination dose-response curve. To calculate the Combination

305 Index (CI), the following equation was used:

306 $CI_{50} = \frac{[\text{Drug 1}] (IC50, \text{ in combination})}{[\text{Drug 1}] (IC50, \text{ alone})} + \frac{[\text{Drug 2}] (IC50, \text{ in combination})}{[\text{Drug 2}] (IC50, \text{ alone})}$

307 The CI was also calculated for CI_{30} (with IC_{30} values) and for CI_{70} (with IC_{70} values). We

308 classified the interaction between the combination of drugs based on the following CI values:

309 CI > 1, Antagonistic; CI = 1, Additive; CI < 1, Synergistic.

310 **Statistical analysis**

311 Student's 2-way ANOVA and two-tailed t-test were calculated using GraphPad Prism 5.0

312 software. *p < 0.05 was considered significant. IC_{50} values were calculated by non-linear

313 regression using GraphPad and 95% confidence intervals were reported.

314

315 **Author Contributions**

316   J.D. and M.A.L designed research; J.D. performed research; J.D. and M.A.L. analyzed

317 data; J.D. and M.A.L. wrote the paper.

318 **Acknowledgements**

326

327 **References**

328 Bernasconi, N.L., Traggiai, E., and Lanzavecchia, A. (2002). Maintenance of serological
329 memory by polyclonal activation of human memory B cells. Science *298*, 2199-2202.

330 Bortnick, A., and Allman, D. (2013). What is and what should always have been: long-lived
331 plasma cells induced by T cell-independent antigens. J Immunol *190*, 5913-5918.

332 Carrington, E.M., Vikstrom, I.B., Light, A., Sutherland, R.M., Londrigan, S.L., Mason, K.D.,
333 Huang, D.C., Lew, A.M., and Tarlinton, D.M. (2010). BH3 mimetics antagonizing restricted
334 prosurvival Bcl-2 proteins represent another class of selective immune modulatory drugs. Proc
335 Natl Acad Sci U S A *107*, 10967-10971.

336 Chou, T.C. (2010). Drug combination studies and their synergy quantification using the Chou-
337 Talalay method. Cancer Res *70*, 440-446.

338 Dave, S.S., Fu, K., Wright, G.W., Lam, L.T., Kluin, P., Boerma, E.J., Greiner, T.C.,
339 Weisenburger, D.D., Rosenwald, A., Ott, G.*, et al.* (2006). Molecular diagnosis of Burkitt's
340 lymphoma. The New England journal of medicine *354*, 2431-2442.

341 Deng, J., Carlson, N., Takeyama, K., Dal Cin, P., Shipp, M., and Letai, A. (2007). BH3 profiling
342 identifies three distinct classes of apoptotic blocks to predict response to ABT-737 and
343 conventional chemotherapeutic agents. Cancer Cell *12*, 171-185.

344 Fischer, U., Janicke, R.U., and Schulze-Osthoff, K. (2003). Many cuts to ruin: a comprehensive
345 update of caspase substrates. Cell Death Differ *10*, 76-100.

346 Gaudette, B.T., Iwakoshi, N.N., and Boise, L.H. (2014). Bcl-xL protein protects from C/EBP
347 homologous protein (CHOP)-dependent apoptosis during plasma cell differentiation. J Biol
348 Chem *289*, 23629-23640.

349 Gupta, V.A., Matulis, S.M., Conage-Pough, J.E., Nooka, A.K., Kaufman, J.L., Lonial, S., and
350 Boise, L.H. (2017). Bone marrow microenvironment-derived signals induce Mcl-1 dependence
351 in multiple myeloma. Blood *129*, 1969-1979.

352 Hawkins, E.D., Turner, M.L., Dowling, M.R., van Gend, C., and Hodgkin, P.D. (2007). A model
353 of immune regulation as a consequence of randomized lymphocyte division and death times.
354 Proc Natl Acad Sci U S A *104*, 5032-5037.

355 Huggins, J., Pellegrin, T., Felgar, R.E., Wei, C., Brown, M., Zheng, B., Milner, E.C., Bernstein,
356 S.H., Sanz, I., and Zand, M.S. (2007). CpG DNA activation and plasma-cell differentiation of
357 CD27- naive human B cells. Blood *109*, 1611-1619.

358 Jellusova, J., Cato, M.H., Apgar, J.R., Ramezani-Rad, P., Leung, C.R., Chen, C., Richardson,
359 A.D., Conner, E.M., Benschop, R.J., Woodgett, J.R.*, et al.* (2017). Gsk3 is a metabolic
360 checkpoint regulator in B cells. Nat Immunol *18*, 303-312.

361 Kelly, G.L., Grabow, S., Glaser, S.P., Fitzsimmons, L., Aubrey, B.J., Okamoto, T., Valente, L.J.,
362 Robati, M., Tai, L., Fairlie, W.D.*, et al.* (2014). Targeting of MCL-1 kills MYC-driven mouse and
363 human lymphomas even when they bear mutations in p53. Genes Dev *28*, 58-70.

364 Klein, U., Klein, G., Ehlin-Henriksson, B., Rajewsky, K., and Kuppers, R. (1995). Burkitt's
365 lymphoma is a malignancy of mature B cells expressing somatically mutated V region genes.
366 Molecular medicine *1*, 495-505.

17

367   Kotschy, A., Szlavik, Z., Murray, J., Davidson, J., Maragno, A.L., Le Toumelin-Braizat, G.,
368   Chanrion, M., Kelly, G.L., Gong, J.N., Moujalled, D.M.*, et al.* (2016). The MCL1 inhibitor S63845
369   is tolerable and effective in diverse cancer models. Nature *538*, 477-482.

370   Kridel, R., Sehn, L.H., and Gascoyne, R.D. (2012). Pathogenesis of follicular lymphoma. J Clin
371   Invest *122*, 3424-3431.

372   Krieg, A.M., Yi, A.K., Matson, S., Waldschmidt, T.J., Bishop, G.A., Teasdale, R., Koretzky, G.A.,
373   and Klinman, D.M. (1995). CpG motifs in bacterial DNA trigger direct B-cell activation. Nature
374   *374*, 546-549.

375   Lessene, G., Czabotar, P.E., Sleebs, B.E., Zobel, K., Lowes, K.N., Adams, J.M., Baell, J.B.,
376   Colman, P.M., Deshayes, K., Fairbrother, W.J.*, et al.* (2013). Structure-guided design of a
377   selective BCL-X(L) inhibitor. Nature chemical biology *9*, 390-397.

378   Leverson, J.D., Zhang, H., Chen, J., Tahir, S.K., Phillips, D.C., Xue, J., Nimmer, P., Jin, S.,
379   Smith, M., Xiao, Y.*, et al.* (2015). Potent and selective small-molecule MCL-1 inhibitors
380   demonstrate on-target cancer cell killing activity as single agents and in combination with ABT-
381   263 (navitoclax). Cell death & disease *6*, e1590.

382   Morales, A.A., Kurtoglu, M., Matulis, S.M., Liu, J., Siefker, D., Gutman, D.M., Kaufman, J.L.,
383   Lee, K.P., Lonial, S., and Boise, L.H. (2011). Distribution of Bim determines Mcl-1 dependence
384   or codependence with Bcl-xL/Bcl-2 in Mcl-1-expressing myeloma cells. Blood *118*, 1329-1339.

385   Nikitin, P.A., Price, A.M., McFadden, K., Yan, C.M., and Luftig, M.A. (2014). Mitogen-induced B-
386   cell proliferation activates Chk2-dependent G1/S cell cycle arrest. PLoS One *9*, e87299.

387   Nikitin, P.A., Yan, C.M., Forte, E., Bocedi, A., Tourigny, J.P., White, R.E., Allday, M.J., Patel, A.,
388   Dave, S.S., Kim, W.*, et al.* (2010). An ATM/Chk2-mediated DNA damage-responsive signaling
389   pathway suppresses Epstein-Barr virus transformation of primary human B cells. Cell Host
390   Microbe *8*, 510-522.

391   Oltersdorf, T., Elmore, S.W., Shoemaker, A.R., Armstrong, R.C., Augeri, D.J., Belli, B.A.,
392   Bruncko, M., Deckwerth, T.L., Dinges, J., Hajduk, P.J.*, et al.* (2005). An inhibitor of Bcl-2 family
393   proteins induces regression of solid tumours. Nature *435*, 677-681.

394   Peperzak, V., Slinger, E., Ter Burg, J., and Eldering, E. (2017). Functional disparities among
395   BCL-2 members in tonsillar and leukemic B-cell subsets assessed by BH3-mimetic profiling.
396   Cell Death Differ *24*, 111-119.

397   Peperzak, V., Vikstrom, I., Walker, J., Glaser, S.P., LePage, M., Coquery, C.M., Erickson, L.D.,
398   Fairfax, K., Mackay, F., Strasser, A.*, et al.* (2013). Mcl-1 is essential for the survival of plasma
399   cells. Nat Immunol *14*, 290-297.

400   Peperzak, V., Vikstrom, I.B., and Tarlinton, D.M. (2012). Through a glass less darkly: apoptosis
401   and the germinal center response to antigen. Immunol Rev *247*, 93-106.

402   Price, A.M., Dai, J., Bazot, Q., Patel, L., Nikitin, P.A., Djavadian, R., Winter, P.S., Salinas, C.A.,
403   Barry, A.P., Wood, K.C.*, et al.* (2017). Epstein-Barr virus ensures B cell survival by uniquely
404   modulating apoptosis at early and late times after infection. Elife *6*.

405   Ranuncolo, S.M., Polo, J.M., Dierov, J., Singer, M., Kuo, T., Greally, J., Green, R., Carroll, M.,
406   and Melnick, A. (2007). Bcl-6 mediates the germinal center B cell phenotype and
407   lymphomagenesis through transcriptional repression of the DNA-damage sensor ATR. Nat
408   Immunol *8*, 705-714.

409 Ryan, J., and Letai, A. (2013). BH3 profiling in whole cells by fluorimeter or FACS. Methods *61*,
410 156-164.

411 Ryan, J., Montero, J., Rocco, J., and Letai, A. (2016). iBH3: simple, fixable BH3 profiling to
412 determine apoptotic priming in primary tissue by flow cytometry. Biol Chem *397*, 671-678.

413 Sarosiek, K.A., Fraser, C., Muthalagu, N., Bhola, P.D., Chang, W., McBrayer, S.K., Cantlon, A.,
414 Fisch, S., Golomb-Mello, G., Ryan, J.A.*, et al.* (2017). Developmental Regulation of
415 Mitochondrial Apoptosis by c-Myc Governs Age- and Tissue-Specific Sensitivity to Cancer
416 Therapeutics. Cancer Cell *31*, 142-156.

417 Shubinsky, G., and Schlesinger, M. (1996). The mechanism of interleukin 4-induced down-
418 regulation of CD38 on human B cells. Cell Immunol *173*, 87-95.

419 Tsujimoto, Y., Cossman, J., Jaffe, E., and Croce, C.M. (1985). Involvement of the bcl-2 gene in
420 human follicular lymphoma. Science *228*, 1440-1443.

421 Victora, G.D., and Nussenzweig, M.C. (2012). Germinal centers. Annu Rev Immunol *30*, 429-
422 457.

423 Vikstrom, I., Carotta, S., Luthje, K., Peperzak, V., Jost, P.J., Glaser, S., Busslinger, M., Bouillet,
424 P., Strasser, A., Nutt, S.L.*, et al.* (2010). Mcl-1 is essential for germinal center formation and B
425 cell memory. Science *330*, 1095-1099.

426 Vo, T.T., Ryan, J., Carrasco, R., Neuberg, D., Rossi, D.J., Stone, R.M., Deangelo, D.J., Frattini,
427 M.G., and Letai, A. (2012). Relative mitochondrial priming of myeloblasts and normal HSCs
428 determines chemotherapeutic success in AML. Cell *151*, 344-355.

429 Wei, M.C., Zong, W.X., Cheng, E.H., Lindsten, T., Panoutsakopoulou, V., Ross, A.J., Roth,
430 K.A., MacGregor, G.R., Thompson, C.B., and Korsmeyer, S.J. (2001). Proapoptotic BAX and
431 BAK: a requisite gateway to mitochondrial dysfunction and death. Science *292*, 727-730.

432 Wenzel, S.S., Grau, M., Mavis, C., Hailfinger, S., Wolf, A., Madle, H., Deeb, G., Dorken, B.,
433 Thome, M., Lenz, P.*, et al.* (2013). MCL1 is deregulated in subgroups of diffuse large B-cell
434 lymphoma. Leukemia *27*, 1381-1390.

435 Wheeler, M.L., and Defranco, A.L. (2012). Prolonged production of reactive oxygen species in
436 response to B cell receptor stimulation promotes B cell activation and proliferation. J Immunol
437 *189*, 4405-4416.

438 Wuilleme-Toumi, S., Robillard, N., Gomez, P., Moreau, P., Le Gouill, S., Avet-Loiseau, H.,
439 Harousseau, J.L., Amiot, M., and Bataille, R. (2005). Mcl-1 is overexpressed in multiple
440 myeloma and associated with relapse and shorter survival. Leukemia *19*, 1248-1252.

441 Youle, R.J., and Strasser, A. (2008). The BCL-2 protein family: opposing activities that mediate
442 cell death. Nature reviews Molecular cell biology *9*, 47-59.

443

444

445
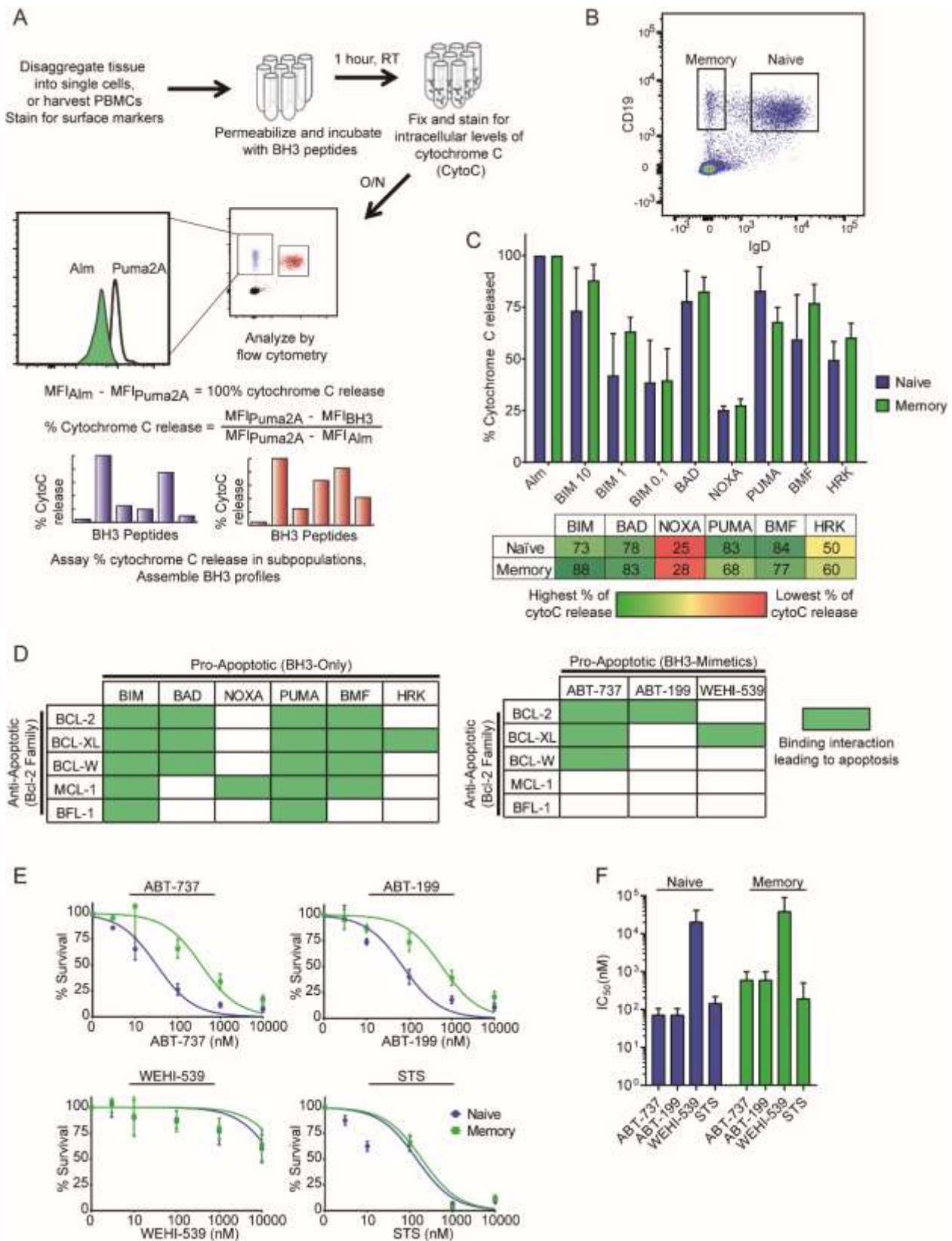
446 **Figure 1. The iBH3 profiles of normal, resting human B cells from the peripheral blood.**

447 A) Schematic of the intracellular BH3 (iBH3) process, including how percentage of cytochrome
448 C release is quantified. B) Representative flow cytometry plot of CD19$^+$ naïve (IgD$^+$) and
449 memory B cells (IgD$^-$) from human peripheral blood mononuclear cells (PBMCs). C) iBH3
450 profiles of naïve and memory B cells from three human donors. Mean and SEM are plotted;
451 mean values are summarized in table below. Percentage of cytochrome C release is normalized
452 to alamethicin (Alm) positive control and Puma2A negative control. BIM 10 - 10µM BIM, BIM 1 -
453 1µM BIM, BIM 0.1 – 0.1µM BIM D) Left, schematic of selective interactions between pro- and
454 anti-apoptotic members of the Bcl-2 protein family and, right, BH3 mimetics and the anti-
455 apoptotic proteins that they inhibit. Green boxes indicate a binding interaction between the two
456 proteins that leads to cytochrome C release. E) Dose-response curves generated from treating
457 PBMCs for 24 hours with ABT-737 (BCL-2, BCL-XL, BCL-W inhibitor; 8 human donors), ABT-
458 199 (BCL-2 inhibitor; 8 human donors), WEHI-539 (BCL-XL inhibitor; 3 human donors) and
459 staurosporine (STS; Naïve, 9 human donors; Memory, 8 human donors), a broad kinase
460 inhibitor that can induce apoptosis. Percent survival is measured as a percentage of DMSO-
461 treated controls. F) Average IC$_{50}$ values with 95% confidence intervals for naïve and memory B
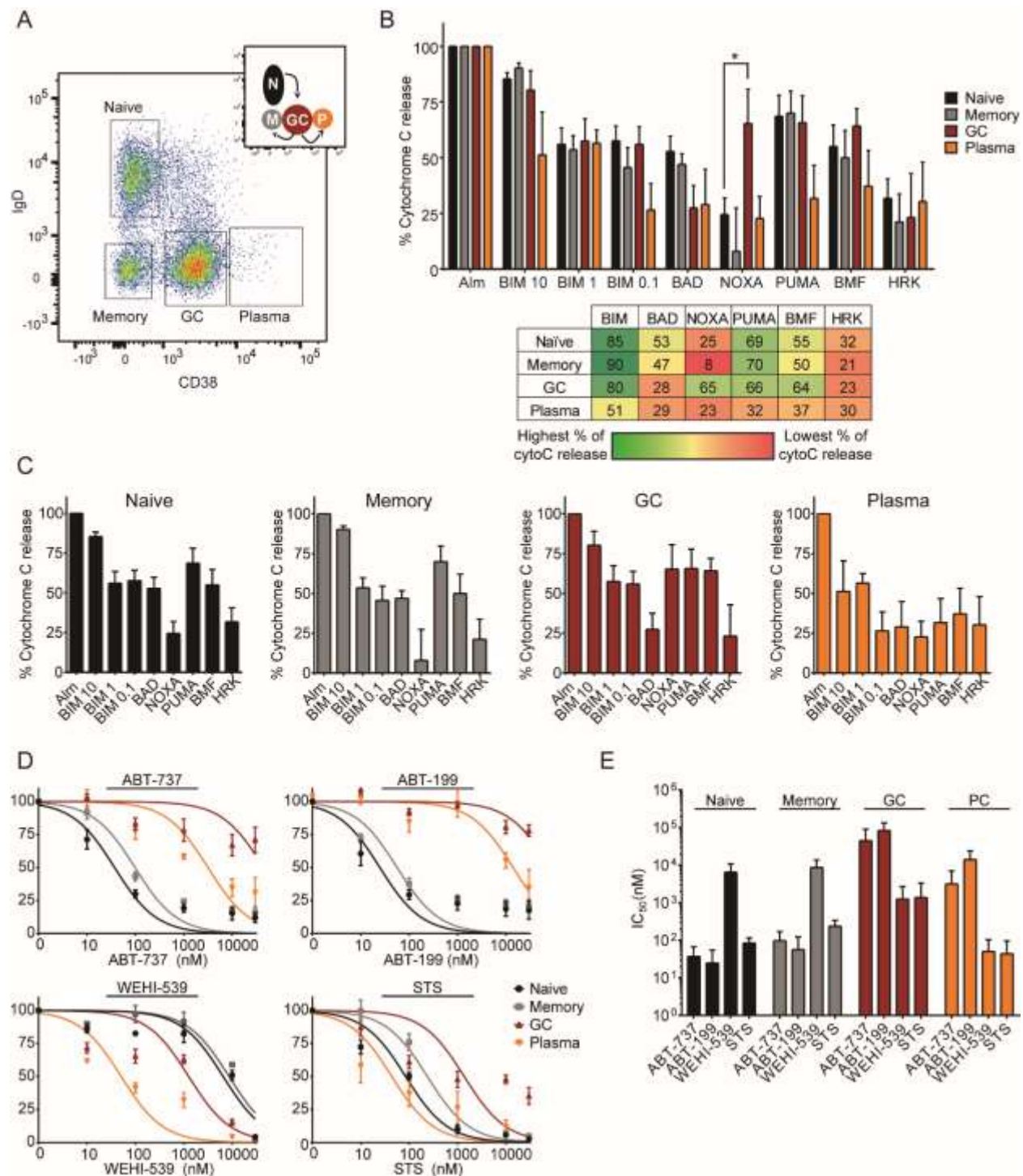462 cells are plotted from (E).

463

464

465

Figure 2. The iBH3 profiles of normal, resting human B cells from tonsillar lymphoid tissue. A) Representative flow cytometry plot of CD19$^+$ B cell subsets found in human tonsillar tissue: naïve (IgD$^+$ CD38$^-$), memory (IgD$^-$ CD38$^-$), germinal center (GC; IgD$^-$ CD38^{mid}), and plasma cells (IgD$^-$ CD38^{hi}). Inset, a color-coded schematic of the GC reaction. B) iBH3 profiles of tonsillar B cell subsets from 4-5 human donors. Mean and SEM are plotted; mean values are summarized in the table below. Percentage of cytochrome C release is normalized to alamethicin (Alm) positive control and Puma2A negative control. In samples treated with Noxa-

474 derived recombinant peptides, * p=0.0467, by unpaired two-tailed Student's t-test. C) Same as
475 in (B), but showing each subset's profile individually. D) Dose-response curves generated from
476 treating eight human donors for 24 hours with ABT-737 (BCL-2, BCL-XL, BCL-W inhibitor; 3
477 human donors), ABT-199 (BCL-2 inhibitor; 3 human donors), WEHI-539 (BCL-XL inhibitor; 3
478 human donors) and staurosporine (STS; 4-6 human donors), a broad kinase inhibitor that can
479 induce apoptosis. Percent survival is measured as a percentage of DMSO-treated controls. E)
480 Average IC_{50} values with 95% confidence intervals for each subset are plotted from (D). Plasma
481 cells, PC.

482

483
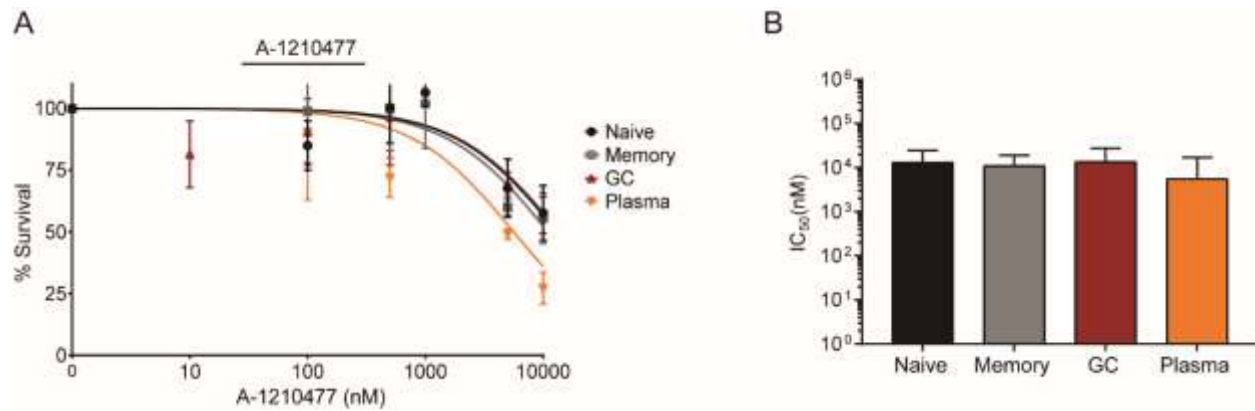
Figure 2 Figure Supplement 1. Tonsillar B cell subsets are largely refractory to the MCL-1 inhibitor A-1210477. A) Dose-response curves generated from treating 5 human donors with A-1210477 (MCL-1 specific BH3 mimetic) for 24 hours. B) Average IC_{50} values with 95% confidence intervals for each subset are plotted from (A).
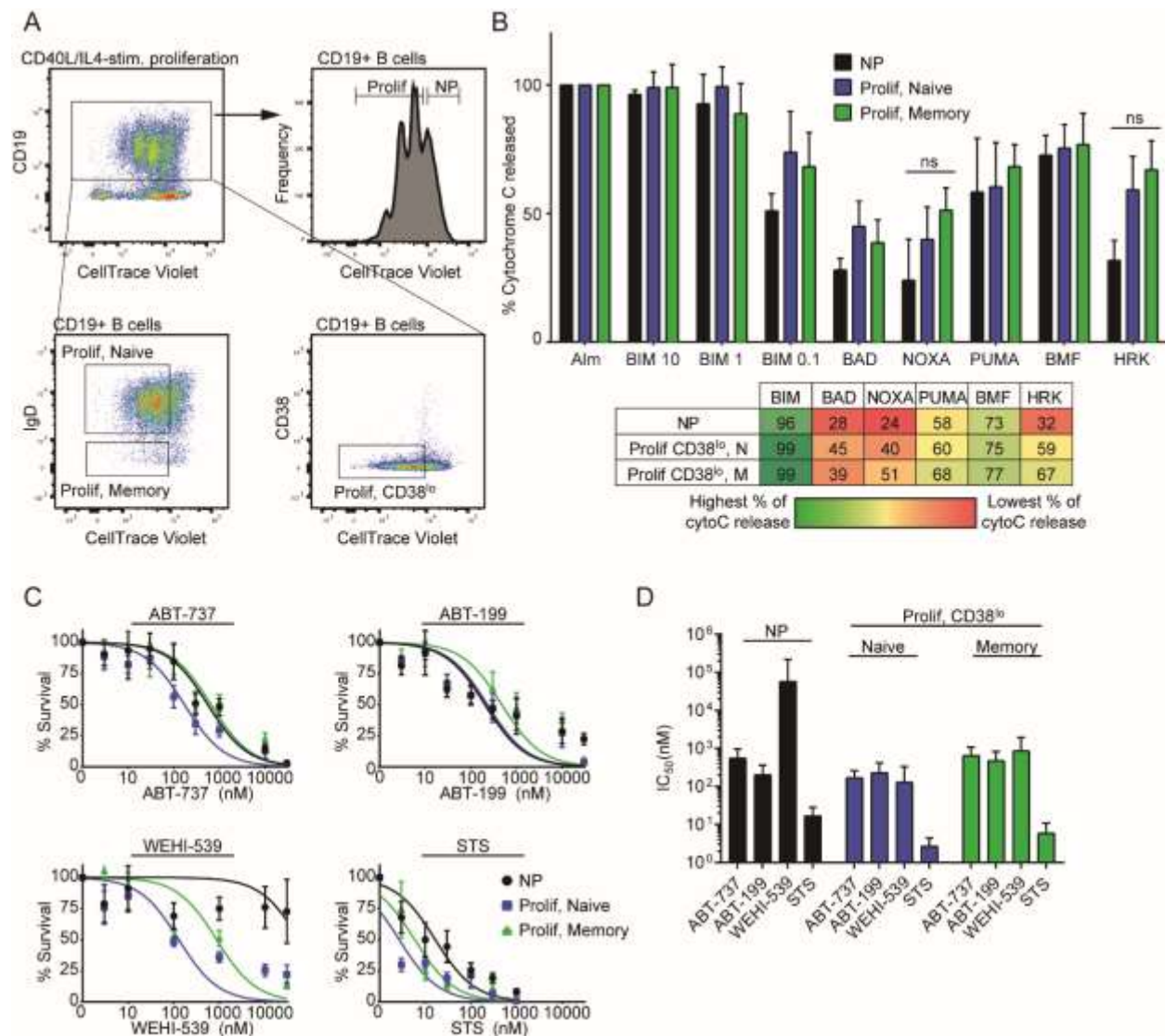
489

Figure 3. Changes in apoptotic regulation in activated, proliferating B cells stimulated by CD40L/IL-4. A) Representative flow cytometry plot of CD19$^+$ B cells that have been stimulated to proliferate by CD40L/IL-4, Day 7 after stimulation. Dilution of CellTrace Violet with each division distinguishes proliferating (Prolif; CTV^{lo}) cells from nonproliferating (NP; CTV^{hi}) cells. Cells that have proliferated the furthest also upregulate CD38 surface expression to some extent, but the size of this population has been inconsistent across donors. Both naïve and memory B cells proliferate in response to CD40L/IL-4 stimulation. B) iBH3 profiles of different subsets of CD40L/IL-4 stimulated B cells from 3-5 human donors. Mean and SEM are plotted; mean values are summarized in the table below. Percentage of cytochrome C release is normalized to alamethicin positive control and Puma2A negative control. ns, not significant by unpaired two-tailed Student's t-test. C) Dose-response curves generated from treating three human donors for 3 days with ABT-737 (6 human donors), ABT-199 (4-9 human donors), WEHI-539 (3 human donors), and STS (6 human donors). D) Average IC$_{50}$ values with 95% confidence intervals for each subset are plotted from (C).
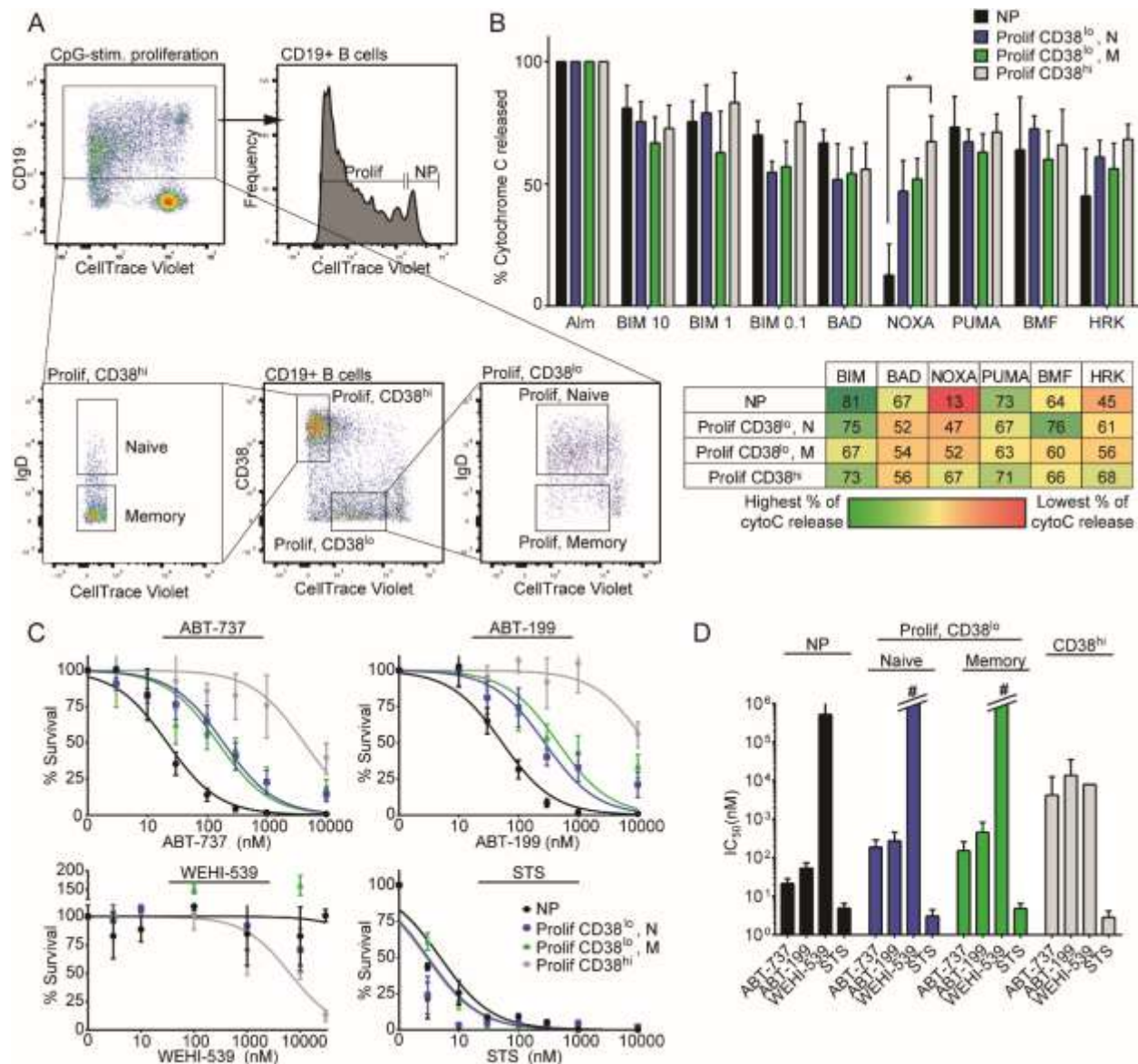
Figure 4. Changes in apoptotic regulation in activated, proliferating B cells stimulated by CpG. A) Representative flow cytometry plot of CD19+ B cells that have been stimulated to proliferate by CpG, Day 6 after stimulation. Dilution of CellTrace Violet with each division distinguishes proliferating (Prolif) cells from nonproliferating (NP) cells. Cells that have proliferated the most also upregulate high CD38 surface expression (CD38hi). Both naïve and memory B cells proliferate in response to CpG stimulation. B) iBH3 profiles of different subsets of CpG-stimulated B cells from 4 human donors. Mean and SEM are plotted; mean values are summarized in the table below. Percentage of cytochrome C release is normalized to alamethicin (Alm) positive control and Puma2A negative control. In samples treated with Noxa-derived peptide, * $p=0.0292$, by unpaired two-tailed Student's t-test. C) Dose-response curves generated from CpG-stimulated PBMCs for 3 days with ABT-737 (5-7 human donors), ABT-199 (5-7 human donors), WEHI-539 (3 human donors), and STS (6-7 human donors). D) Average IC_{50} values with 95% confidence intervals for each subset are plotted from (C). #, for these subsets, there is no detectable sensitivity and therefore no calculable IC_{50} value.
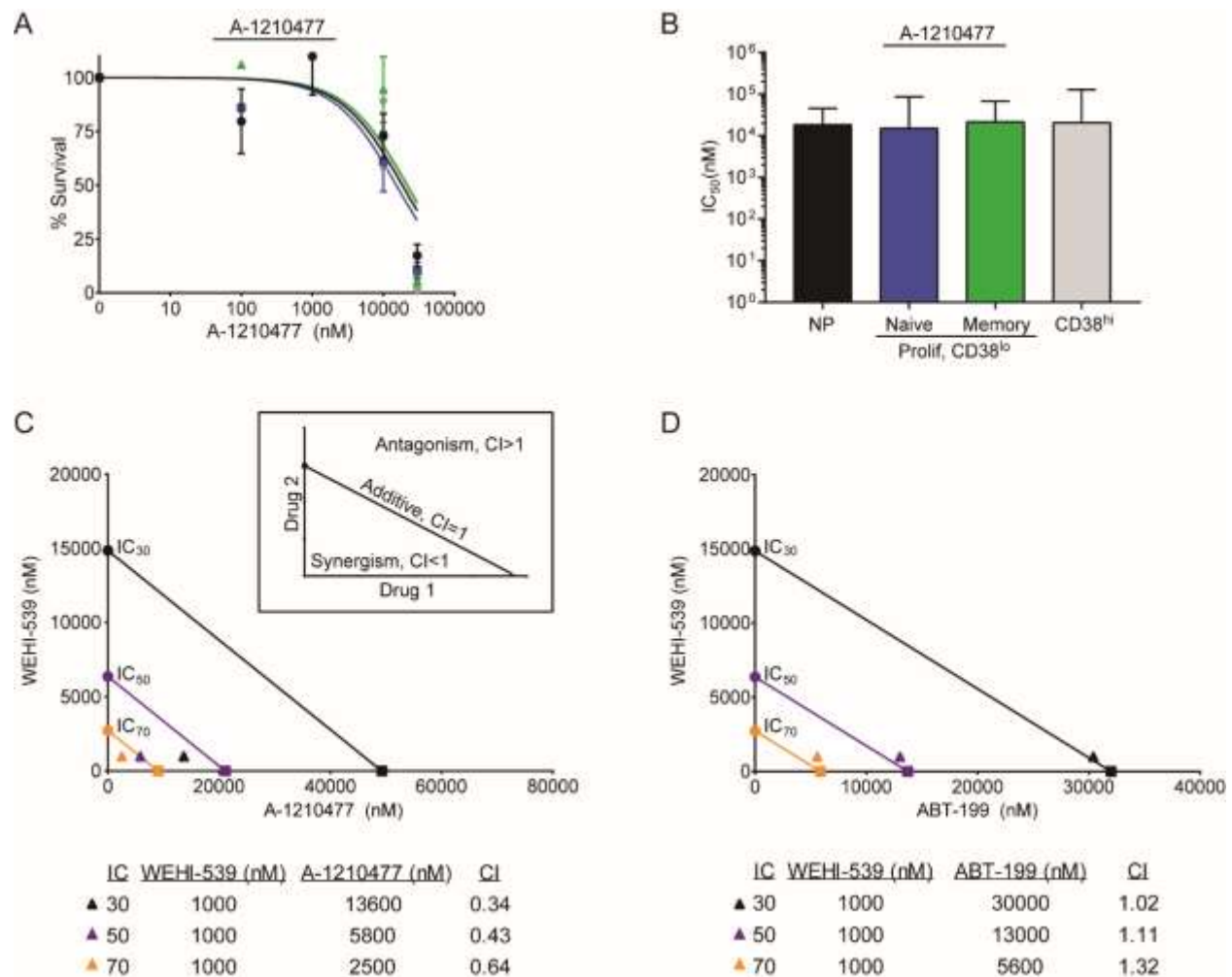
Figure 4 Figure Supplement 1. Combined BCL-XL and MCL-1 inhibition is cytotoxic to the CD38^{hi} subset of CpG-stimulated B cells. A) Dose-response curves generated from treating CpG-stimulated PBMCs for 3 days with A1210477 (3 human donors). B) Average IC$_{50}$ values with 95% confidence intervals for each subset are plotted from (A). C) Isobologram generated from treating CpG-stimulated PBMCs for 3 days with WEHI-539 (from Figure 4C), A1210477 (from Figure 4 Figure Supplement 1A), and in combination. IC$_{30}$ (black), IC$_{50}$ (purple), and IC$_{70}$ (orange) values are plotted for WEHI-539 alone (●), A1210477 alone (■), and A1210477 in combination with 1000nM WEHI-539 (▲). Combination index (CI) values are listed below. Inset, a schematic of the combination index (CI) values of synergistic, additive, and antagonistic interactions and where they fall on an isobologram. D) Isobologram generated from treating CpG-stimulated PBMCs for 3 days with WEHI-539 (from Figure 4C), ABT-199 (from Figure 4C) and in combination. IC$_{30}$ (black), IC$_{50}$ (purple), and IC$_{70}$ values are plotted for WEHI-539 alone (●), ABT-199 alone (■), and ABT-199 in combination with 1000nM WEHI-539 (▲). Combination index (CI) values are listed below.

27